Radiative electron capture by channeled ions

J. M. Pitarke
Fisika Teorikoa Saila, Zientzi Fakultatea, Euskal Herriko Unibertsitatea, 644 Posta kutxatila, 48080 Bilbo, Basque Country, Spain

R. H. Ritchie
Oak Ridge National Laboratory, P.O. Box 2008, Oak Ridge, Tennessee 37831-6123 and The University of Tennessee, Department of Physics, Knoxville, Tennesee 37996

P. M. Echenique
Materialen Fisika Saila, Kimika Fakultatea, Euskal Herriko Unibertsitatea, 1072 Posta kutxatila, 20080 Donostia, Basque Country, Spain

(Received 30 May 1990)

Much experimental data have been accumulated relative to the emission of photons accompanying electron capture by swift, highly stripped channeled ions. Recent data suggest that the photon energies may be less than that expected from simple considerations of transitions from the valence band of the solid to hydrogenic states on the moving ion. We have studied theoretically the impact-parameter dependence of the radiative-electron-capture process, including the effect of the ion's wake and capture from inner shells of the solid on the photon-emission probability, and using a statistical local-density approach. Numerical comparisons of our results with experiment are made.

I. INTRODUCTION

Schnopper *et al.*[1] first observed the process of charge transfer from a target atom to a highly stripped fast ion in condensed matter accompanied by the emission of a photon. Since then, this radiative-electron-capture (REC) process has been the subject of much theoretical and experimental effort,[2–12] since it could become a significant tool in the study of the momentum distribution of target electrons.

The REC process contributes only in a very small way to the total production of radiation when swift ions cross the matter; however, as pointed out by Appleton *et al.*,[6] it becomes more important and amenable to interpretation when the bombarding ions are channeled through the solid, since in these conditions the ions never approach closer than 0.1 or 0.2 Å to target atoms. Thus, the yield of characteristic x rays is very much smaller than that observed when the beam is incident on the crystal in a random direction. Furthermore, it has been shown that channeled ions in thin foils have frozen charge states, and although nonradiative electron capture is the dominant mechanism for charge transfer, in ion channeling the inhibition of close collisions makes the radiative process relatively more important.

The purpose of this paper is to extend previous theoretical approaches[4,9] and to study the impact-parameter dependence of the REC process as well as the effect of capture from inner shells of the solid. We present an interpretation of recent experimental data,[13] which suggest that REC photon energies may be less than that expected from simple considerations of transitions from the valence band of the solid to hydrogenic states of the moving ion. Measured peak-energy positions, widths, and cross sections of the emitted radiation are compared to calculations made for the channeling mode.

II. THEORY

We consider a solid through which a swift, stripped ion of charge Z_1 and velocity $\mathbf{v}$ passes, and assume that it captures an electron accompanied by the emission of a single photon. Treating the ion as infinitely massive, and proceeding nonrelativistically, we work in the projectile frame where the center-of-mass motion generates no current, so that the possibility of spurious radiation does not arise.[14] Unless otherwise stated, atomic units are used throughout.

The probability per unit energy and unit solid angle for capturing a target electron from the initial state, represented by $\varphi_i(\mathbf{r})$, into the final bound state, represented by $\varphi_j(\mathbf{r})$, in a collision at impact parameter $\mathbf{b}$ with emission of a photon of polarization $\boldsymbol{\lambda}$ and propagation vector $\mathbf{k}$ is found by treating the electromagnetic field as a small perturbation and using first-order perturbation theory.[15] We have

$$\left[\frac{d^3\gamma}{dE\,d\Omega}\right]_{\mathbf{b},\boldsymbol{\lambda}}=\frac{E^2}{c^3}|f|^2\ , \tag{1}$$

where $E=ck$ is the photon energy, c is the velocity of light, and the amplitude f is given by

$$f=(2\pi i\sqrt{E}\,)^{-1}\times\int dt\,e^{i\omega t}\langle\varphi_f(\mathbf{r})|e^{-i\mathbf{k}\cdot\mathbf{r}}\boldsymbol{\lambda}\cdot\boldsymbol{\nabla}|\varphi_i(\mathbf{r}+\mathbf{b}+\mathbf{v}t)e^{-i\mathbf{v}\cdot\mathbf{r}}\rangle\ , \tag{2}$$

with

$$\omega = E + E_f - E_i - \tfrac{1}{2}v^2 \ . \tag{3}$$

E_i and E_f are the initial and final stationary-state energies, referring to the target and to the ion, respectively. After Fourier transformation of the wave functions to the momentum representation, we find

$$f = E^{-1/2} \int d\mathbf{q}\, \delta(\omega + \mathbf{q}\cdot\mathbf{v}) \boldsymbol{\lambda}\cdot(\mathbf{q}-\mathbf{v}) e^{i\mathbf{q}\cdot\mathbf{b}} \times \tilde{\varphi}_f^*(\mathbf{q}-\mathbf{v}-\mathbf{k}) \tilde{\varphi}_i(\mathbf{q}) \ . \tag{4}$$

If we specialize to the situation in which the electron is captured to the lowest state, that is, to a K-shell orbital of the ion, we have[16]

$$\varphi_f(\mathbf{r}) = (\alpha^3/\pi)^{1/2} e^{-\alpha r} \ , \tag{5}$$

with

$$\alpha = (-2E_f)^{1/2} \ . \tag{6}$$

It is interesting to remark that the enhancement of the mean electron density of the polarized medium induces a potential at the site of the projectile given, in the linear approximation, by[17]

$$\lim_{r\to 0} \left[\Phi(\mathbf{r}) - \frac{Z_1}{r} \right] = -\frac{\pi Z_1 \omega_p}{2v} \ , \tag{7}$$

where $\Phi(\mathbf{r})$ is the total wake potential of the projectile moving in the medium, and ω_p is the plasmon frequency

$$\omega_p = (3/r_s^3)^{1/2} \ , \tag{8}$$

r_s being the equivalent one-electron radius of the electron gas, at the position of the ion. Consequently, the energy eigenvalue for the lowest state of the hydrogenlike moving ion should be

$$E_f = -\tfrac{1}{2}Z_1^2 + \frac{\pi Z_1 \omega_p}{2v} \ . \tag{9}$$

A. Capture of an electron from a bound state in the solid

Suppose that electrons in the solid and near the center of a channel may be represented by the orbital

$$\varphi_i(\mathbf{r}) = (\beta^3/\pi)^{1/2} e^{-\beta r} \ , \tag{10}$$

with

$$\beta = (-2E_i)^{1/2} \ , \tag{11}$$

E_i being the binding energy of the electron in the lattice, which may be taken to be a few eV, and r the distance from a lattice atom to the ion. This is a very schematic form of the wave function in an interior region of the solid that will be improved later on.

Introducing the Fourier transforms of the wave functions (5) and (10) into (4), we find

$$f = \frac{2^3(\alpha\beta)^{5/2}}{\pi^2\sqrt{E}} \int d\mathbf{q}\, \boldsymbol{\lambda}\cdot(\mathbf{q}-\mathbf{v}) \delta(\mathbf{q}\cdot\mathbf{v}+\omega) \times \frac{e^{i\mathbf{q}\cdot\mathbf{b}}}{[\alpha^2+(q')^2]^2(\beta^2+q^2)^2} \ , \tag{12}$$

where

$$\mathbf{q}' = \mathbf{q} - \mathbf{v} - \mathbf{k} \ . \tag{13}$$

Introducing (12) into (1), choosing the z axis in the direction of $\mathbf{v}$, taking $(\mathbf{Q}, q_z)$, summing over the polarization index, λ, and transferring to the laboratory frame, we find in the dipole approximation the following expression for the probability per unit energy and unit solid angle for emission of a photon of energy E at θ with respect to the beam direction after a collision at impact parameter $\mathbf{b}$:

$$\left[\frac{d^3\gamma}{dE\, d\Omega} \right]_b = \frac{2^6(\alpha\beta)^5 E}{\pi^4 c^3 v^2} \sum_{\lambda} \left| \int d\mathbf{Q} \frac{\boldsymbol{\lambda}\cdot(\mathbf{Q}+\mathbf{Q}_\alpha) e^{i\mathbf{Q}\cdot\mathbf{b}}}{(\alpha^2+Q^2+Q_\alpha^2)^2(\beta^2+Q^2+Q_\beta^2)^2} \right|^2 \ , \tag{14}$$

where

$$\mathbf{Q}_\alpha = \frac{1}{v^2}[-E_f + E_i - \tfrac{1}{2}v^2 - E(1 - v\cos\theta/c)]\mathbf{v} \tag{15}$$

and

$$\mathbf{Q}_\beta = \frac{1}{v^2}[-E_f + E_i + \tfrac{1}{2}v^2 - E(1 - v\cos\theta/c)]\mathbf{v} \ . \tag{16}$$

In particular, for emission of a photon at $\theta = 0$ with respect to the beam direction, we have

$$\left[\frac{d^3\gamma}{dE\, d\Omega} \right]_b (\theta=0) = \frac{2^8(\alpha\beta)^5 E}{\pi^2 c^3 v^2} \left| \int_0^\infty dQ \frac{Q^2 J_0(Qb)}{(\alpha^2+Q^2+Q_\alpha^2)^2(\beta^2+Q^2+Q_\beta^2)^2} \right|^2 \ , \tag{17}$$

and for emission of radiation at $\theta \gg 1$, one may write

$$\left[\frac{d^3\gamma}{dE\, d\Omega} \right]_b (\theta \gg 1) \approx \frac{2^8(\alpha\beta)^5 E \sin^2\theta}{\pi^2 c^3} \left| \int_0^\infty dQ \frac{Q J_0(Qb)}{(\alpha^2+Q^2+Q_\alpha^2)^2(\beta^2+Q^2+Q_\beta^2)^2} \right|^2 \ , \tag{18}$$

since the momentum wave functions $\varphi_{ij}(\mathbf{q})$ are peaked around $\mathbf{q}=0$. J_0 represents the zero-order Bessel function of the first kind.

We give in Fig. 1 the REC spectrum calculated from Eq. (18) for 160-MeV bombarding bare sulphur ions channeled through silicon, with $\theta=46.5°$ as in the experiment of Ref. 13, and $b=1.5$ Å. In this calculation, the final stationary-state energy has been corrected according to Eq. (9) using the equivalent one-electron radius of an electron gas of valence electron density equal to the total electron density in the center of the channel ($b=1.5$ Å), i.e., $r_s=2.15$ a.u. (see Fig. 3).

If we neglect the difference between the vacuum energy and the actual energy of electrons in the target, as well as the shift in the binding energy of an electron to the projectile due to polarization of the medium, the REC energy is given by

$$E_{\mathrm{REC}}=\tfrac{1}{2}v^2+\tfrac{1}{2}Z_1^2 \ . \tag{19}$$

Figure 1 shows that the peak energy closely approximates the REC energy of Eq. (19), though it is slightly smaller due to the wake correction in the center of the channel.

The REC half widths calculated from Eq. (18) are given in Fig. 2, as a function of the impact parameter b for the same conditions as in Fig. 1. Notice that the photon energy distribution broadens as the impact parameter decreases; this is consistent with the use of a local-density approximation, whereby the initial momentum distribution of target electrons may be expected to be wider as the impact parameter decreases, as will be shown in the next section.

B. Capture in the local-density approximation

The electronic structures of crystalline solids of interest in REC experiments are intricate and tedious to calculate by state-of-the-art numerical methods. Even if known, the representation of such structures in terms of orbitals such as in the simple example displayed in Sec. II A above would be difficult and time consuming. Here we simplify REC calculations considerably by using the local-density approximation. We assume that each volume element of the solid encountered by the ion in its channeling trajectory constitutes an independent electron gas at the total local electron density, $n(\mathbf{r})$. The local Fermi energy is taken to be

$$E_F(\mathbf{r})=\frac{[3\pi^2 n(\mathbf{r})]^{2/3}}{2} \ , \tag{20}$$

when capture occurs from the vicinity of $\mathbf{r}$ in the solid. Then we make the statistical average of the local REC probability derived in this way over all possible channeling trajectories of the ion.

1. Plane waves

Firstly, we assume in this approximation that the wave functions of electrons in a given part of the solid are plane waves

$$\varphi_i(\mathbf{r})=\frac{1}{\sqrt{V}}e^{i\mathbf{q}\cdot\mathbf{r}} \ , \tag{21}$$

where $\mathbf{q}$ represents the initial momentum of the target electron in the laboratory frame.

After introducing Fourier transforms of the wave functions (5) and (21) into Eq. (4), one finds

$$f=\left[\frac{2^4\alpha^5}{EV\pi}\right]^{1/2}\frac{\boldsymbol{\lambda}\cdot(\mathbf{q}-\mathbf{v})e^{i\mathbf{q}\cdot\mathbf{b}}}{[\alpha^2+(\mathbf{q}-\mathbf{v}-\mathbf{k})^2]^2}\int_{-\infty}^{\infty}dt\, e^{j(\omega+\mathbf{q}\cdot\mathbf{v})t} \ ; \tag{22}$$

then substituting Eq. (22) into Eq. (1), and summing over the polarization index and over initial states of target electrons, we find the transition rate per unit energy and unit solid angle for emission of a photon of energy E and propagation vector $\mathbf{k}$ to be

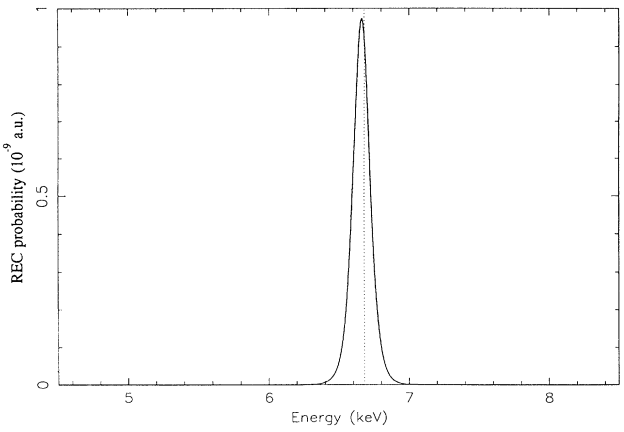

FIG. 1. REC probability per unit energy and unit solid angle obtained from Eq. (18) for 160-MeV bombarding bare sulfur ions, when capture occurs of electrons at 1.5 Å from the nearest atom in the crystal. The vertical dotted line refers to the REC energy of Eq. (19).

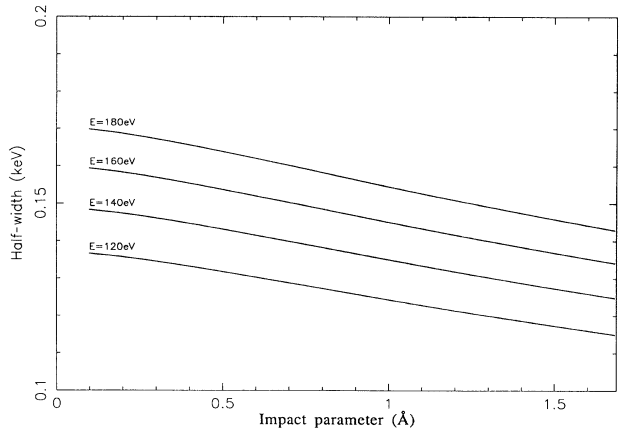

FIG. 2. Half widths calculated from Eq. (18), as a function of the impact distance, for incident ion energies from 120 to 180 MeV.

$$\frac{d^3\dot{\gamma}}{dE\,d\Omega}=\frac{2^5\alpha^5E}{c^3V}\sum_i\frac{|\mathbf{k}\times(\mathbf{q}-\mathbf{v})|^2/k^2}{[\alpha^2+(\mathbf{q}-\mathbf{v}-\mathbf{k})^2]^4}\delta(\omega+\mathbf{q}\cdot\mathbf{v})\ , \tag{23}$$

where we have substituted the identity[18]

$$\sum_\lambda|\boldsymbol{\lambda}\cdot(\mathbf{q}-\mathbf{v})|^2=|\mathbf{k}\times(\mathbf{q}-\mathbf{v})|^2/k^2 \tag{24}$$

and

$$\omega+\mathbf{q}\cdot\mathbf{v}=E+E_f+E_F-\tfrac{1}{2}(\mathbf{q}-\mathbf{v})^2\ , \tag{25}$$

where E_i is the energy of the electron referenced to the vacuum level and E_F represents the local Fermi energy of Eq. (20), which accounts for the fact that electrons at small r tend to be bound in the solid more strongly than those at larger values of r.

The first summation in (23) runs over initial states of the target electron; transforming this sum to an integral covering a Fermi sphere of electrons, incorporating a factor of 2 for the possible spin states, and transforming to the laboratory frame, we find, after some algebra, the differential inverse mean free path (DIMFP) per unit energy and unit solid angle for emission of a photon with energy E at θ with respect to the incident beam as

$$\frac{d\mu}{dE\,d\Omega}=\frac{\alpha^5E}{2\pi^3c^3v^2}\int_{q_{\min}}^{q_{\max}}dq\,q\int_0^{2\pi}d\varphi\frac{[(q\mu-v)\sin\theta-q\nu\cos\theta\cos\varphi]^2+\nu^2q^2\sin^2\varphi}{\left[E_F+E'\left[1-\frac{q}{c}\rho+\frac{v}{c}\cos\theta+\frac{E}{2c^2}\right]\right]^4}\ , \tag{26}$$

when

$$E_1-E_f-2\sqrt{E_1E_F}\le E'\le E_1-E_f+2\sqrt{E_1E_F}\ , \tag{27}$$

and zero, otherwise. In these expressions,

$$q_{\min}=\sqrt{2(E_f+E_F+E')}-\sqrt{2E_1}\ , \tag{28}$$

$$q_{\max}=\min(\sqrt{2E_F},\sqrt{2(E_f+E_F+E')}+\sqrt{2E_1})\ , \tag{29}$$

$$\mu=\frac{1}{qv}[\tfrac{1}{2}q^2-(E_f+E_F+E')+E_1]\ , \tag{30}$$

$$\nu=(1-\mu^2)^{1/2}\ , \tag{31}$$

$$\rho=\mu\cos\theta+\nu\sin\theta\cos\varphi\ , \tag{32}$$

$$E_1=\tfrac{1}{2}v^2\ , \tag{33}$$

and

$$E'=E(1-v\cos\theta/c)\ . \tag{34}$$

If the dipole approximation is made, thus neglecting $\mathbf{k}$ in comparison with $\mathbf{q}$ and $\mathbf{v}$, one obtains

$$\frac{d\mu}{dE\,d\Omega}=\frac{\alpha^5E}{4\pi^2c^3}\frac{C_1(E_{\max}-E_{\min})+C_2(E_{\max}^2-E_{\min}^2)+C_3(E_{\max}^3-E_{\min}^3)}{E_1(E_F+E')^4}\ , \tag{35}$$

where

$$C_1=\frac{(E_f+E_F+E'-E_1)^2}{2E_1}(\sin^2\theta-2\cos^2\theta)+4(E_f+E_F+E')\sin^2\theta\ , \tag{36}$$

$$C_2=-\frac{E_f+E_F+E'+E_1}{2E_1}(\sin^2\theta-2\cos^2\theta)\ , \tag{37}$$

$$C_3=\frac{1}{6E_1}(\sin^2\theta-2\cos^2\theta)\ , \tag{38}$$

$$E_{\min}=\tfrac{1}{2}q_{\min}^2\ , \tag{39}$$

and

$$E_{\max}=\tfrac{1}{2}q_{\max}^2\ . \tag{40}$$

Integrating Eq. (35) over all directions of photon emission, one finds the DIMFP per unit energy for emission of a photon with energy E as

$$\frac{d\mu}{dE}=\frac{2^4\alpha^5E}{3\pi c^3v^2}\frac{(E_f+E_F+E)(E_{\max}-E_{\min})}{(E_F+E)^4}\ . \tag{41}$$

2. *Coulombic waves*

Alternatively, we may assume, in the local-density approximation, that each electron undergoing capture from the solid experiences the full Coulomb field of the projec-

tile, that is, that target electrons in a given part of the solid are in a continuum hydrogenic state of the bare bombarding ion,

$$\varphi_i(\mathbf{r})=\frac{1}{\sqrt{V}}\frac{1}{2q}\sum_{l=0}^{\infty}(2l+1)i^l e^{i\delta_l}R_l(q,r)P_l(\cos\theta)\ , \tag{42}$$

where $\mathbf{q}$ represents, as before, the initial momentum of the electron, the quantities R_l and P_l represent the radial solution of the Schrödinger equation and the Legendre polynomials, respectively, and θ is the angle between $\mathbf{q}$ and $\mathbf{r}$.

Making use of the fact that in the dipole approximation only those continuum eigenfunctions with $l=1$ contribute, we find in this approximation the following result for the transition rate per unit energy and unit solid angle for emission of a photon of propagation vector $\mathbf{k}$:

$$\frac{d^3\dot{\gamma}}{dE\,d\Omega}=\frac{2^6\pi\alpha^6E}{c^3V}\sum_i\frac{|\mathbf{k}\times(\mathbf{q}-\mathbf{v})|^2 f(\sqrt{-E_f/(E_f+E_F+E)})/k^2}{(\mathbf{q}-\mathbf{v})^3[\alpha^2+(\mathbf{q}-\mathbf{v})^2]^3}\delta(\omega+\mathbf{q}\cdot\mathbf{v})\ , \tag{43}$$

where the argument of the δ function is given by Eq. (25), and

$$f(x)=\frac{e^{-4x\tan^{-1}(1/x)}}{1-e^{-2\pi x}}\ . \tag{44}$$

In particular, setting the Fermi energy equal to zero, thus the only contribution to the sum over initial states coming from $q=0$, and integrating over all directions and energies of the emitted radiation yields the Bethe-Salpeter cross section for radiative recombination.[19]

Now transforming the sum of Eq. (43) to an integral covering a Fermi sphere of target electrons, incorporating a factor of 2 for the possible spin states, and transforming to the laboratory frame, one finds

$$\frac{d\mu}{dE\,d\Omega}=\frac{\alpha^6E}{2^{3/2}\pi c^3}\frac{C_1(E_{\max}-E_{\min})+C_2(E_{\max}^2-E_{\min}^2)+C_3(E_{\max}^3-E_{\min}^3)}{E_1(E_f+E_F+E')^{3/2}(E_F+E')^3}f(\sqrt{-E_f(E_f+E_F+E')})\ , \tag{45}$$

where C_1, C_2, C_3, $E_{\min}$, and $E_{\max}$ are given by Eqs. (36), (37), (38), (39), and (40), respectively, and E' is the energy of the emitted radiation with respect to the ion frame, which is given by Eq. (34).

Integrating Eq. (45) over all directions of the emitted radiation, one finds

$$\frac{d\mu}{dE}=\frac{2^{7/2}\alpha^6E}{3c^3}\frac{(E_{\max}-E_{\min})f(\sqrt{-E_f/(E_f+E_F+E)})}{E_1(E_f+E_F+E)^{1/2}(E_F+E)^3}\ . \tag{46}$$

3. *Statistical model for channeled ions*

With the aim of interpretating the available experimental data, we are interested in the dependence of REC probabilities on photon energy for a given direction of emission. Therefore, we consider expressions (26), (35), and (45) for the local DIMFP per unit energy and unit solid angle in a given part of the solid, and then we employ a statistical approximation.

Assuming that capture from an infinitesimal volume element of the solid can be calculated by attributing the local Fermi energy of Eq. (20) to electrons in that volume element, and that channeled ions sample on straight-line trajectories all portions of the Wigner-Seitz sphere corresponding to impact parameters greater than a given $b_{\min}$, we follow Ref. 9 and write the statistical average of the DIMFP per unit energy and unit solid angle as[9,20]

$$\left\langle\frac{d\mu}{dE\,d\Omega}\right\rangle=\frac{3}{r_{\rm WS}^3}\int_{b_{\min}}^{r_{\rm WS}}dr\,r(r-b_{\min})\frac{d\mu}{dE\,d\Omega}[E_F(r)]\ , \tag{47}$$

where $r_{\rm WS}$ is the Wigner-Seitz radius, and the local DIMFP per unit energy and unit solid angle is given by Eqs. (26), (35), or (45), depending on whether the dipole approximation is made and whether plane waves or Coulombic waves of target electrons are used. The total electron density in this expression is computed from a relativistic Hartree-Fock program using the Wigner-Seitz boundary condition,[21] thus obtaining the local Fermi energy from Eq. (20). Figure 3 shows a plot against r of the local equivalent one-electron radius computed in this way for silicon.

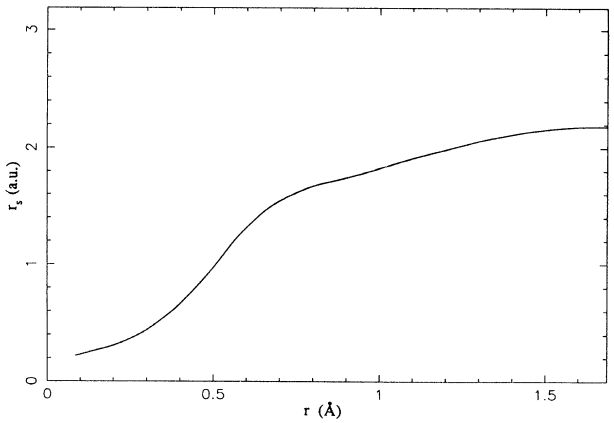

FIG. 3. The equivalent one-electron radius $r_s(r)$ plotted vs position in the Wigner-Seitz cell for silicon, as calculated using a relativistic Hartree-Fock approach (Ref. 21).

III. RESULTS

In the present section we consider the REC spectrum for collision of 100–200-MeV S^{16+} ions channeling through a silicon target, when photons are emitted at 46.5° with respect to the beam direction. Comparisons of our results with the experimental data of Vane *et al.*[13] are made.

We give in Fig. 4(a) the REC spectrum calculated from Eqs. (26), (35), and (45), for 160-MeV bombarding bare sulphur ions and the local electron density of Fig. 3 corresponding to capture of electrons at 1.5 Å from the nearest atom in the crystal. The solid line has been calculated using initial-state plane waves, in the dipole approximation. The dotted line has been obtained employing plane waves, without the dipole approximation, from Eq. (26), and the dashed line has been calculated for initial-state Coulombic wave functions, in the dipole approximation. It is interesting to remark that Eqs. (26) and (35) predict essentially the same dependence of REC probabilities on photon energy, although the results differ somewhat in magnitude. This figure also shows that assuming Coulomb continuum wave functions rather than plane waves for the initial states gives somewhat relatively greater REC probabilities for small photon energies; the energy of the REC peak is also slightly smaller. We should mention that this effect happens to be more important as the impact parameter decreases.

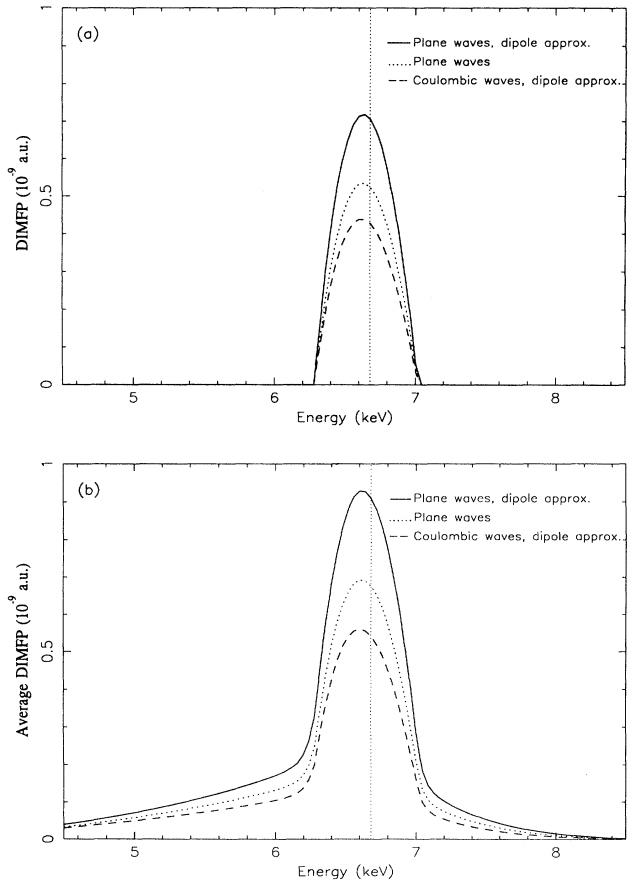

FIG. 4. REC spectra obtained for 160-MeV bombarding bare sulfur ions. (a) Local DIMFP per unit energy and unit solid angle calculated from Eqs. (26) (dotted curve), (35) (solid curve), and (45) (dashed curve), when capture occurs of electrons at 1.5 Å from the nearest atom in the crystal. (b) Average DIMFP per unit energy and unit solid angle calculated from Eq. (47), for $b_{\min}=0.1$ Å and the local DIMFP's of Eqs. (26) (dotted curve), (35) (solid curve), and (45) (dashed curve). The vertical dotted line refers to the REC energy of Eq. (19).

It has been found that for small impact parameters the DIMFP peak energy deviates importantly from the energy predicted by Eq. (19). This deviation is originated in two different ways: On the one hand, the wake correction to the binding energy of the captured electron gets more important as r decreases, and, on the other hand, inner-shell electrons are more strongly bound to the solid; this effect is slightly enhanced as a result of the fact that emission probabilities get slightly greater as the energy decreases, especially when the initial Coulombic wave functions are considered. These results are favorably related to the REC deficit observed in recent experimental data.[13]

In order to compare our theoretical results with experiment, we compute the statistical average of the local DIMFP by means of Eq. (47). Figure 4(b) exhibits plots of the average DIMFP per unit energy and unit solid angle when the minimum impact parameter is taken to be $b_{\min}=0.1$ Å; the local DIMFP's have been calculated from Eqs. (26), (35), and (45), with the distance-dependent local electron density of Fig. 3. Comparing Figs. 4(a) and 4(b) we find that the contribution of capture from inner shells gives rise to a small shift in the peak energy comparable to the experimentally observed REC deficit. In order to illustrate this, the average DIMFP peak energies deduced from Eq. (47) for $b_{\min}=0.1$ Å are plotted in Fig. 5(a) versus the energy of the incident ion, together with the experimentally measured peak energies of Ref. 13 and the REC energies of Eq. (19).

It appears from Fig. 5(a) that the calculated peak energies are systematically smaller than the REC energies calculated from Eq. (19) by about 80 eV, in approximate agreement with the experimental results. Representing target electrons by Coulombic wave functions gives rise to slightly smaller peak energies, as discussed above; this can be due to the fact that in this case the increase in the emission probability as the energy decreases becomes more important. On the other hand, it may be shown that making use of the dipole approximation does not affect appreciably the peak-energy positions obtained employing plane waves.

The origin of the REC deficit obtained in this approximation is twofold, as discussed above. As the impact parameter decreases, thus increasing the total electron density, the wake correction to the binding energy of the captured electron is enhanced, on the one hand, and the initial momentum distribution of target electrons gets wider, on the other hand. These two contributions to the energy deficit are shown separately in Fig. 5(b), as a function of the energy of projectiles, for $b_{\min}=0.1$ Å; the dashed line represents the contribution to the energy deficit due to the broadening of the momentum distribu-

tion, the dotted line represents the contribution from the wake correction to the binding energy of the captured electron, and the solid line represents the total energy deficit.

Radiative electron-capture half widths calculated from average REC distributions described by Eq. (47) are found to be wider as the minimum impact parameter decreases, as one might expect. We have calculated, also, widths of these distributions as a function of the incident ion energy, and plotted them in Fig. 6 for different minimum impact parameters, together with the experimental results of Ref. 13. The theoretical values are somewhat larger than the experimental ones, but the energy dependences are nearly the same.

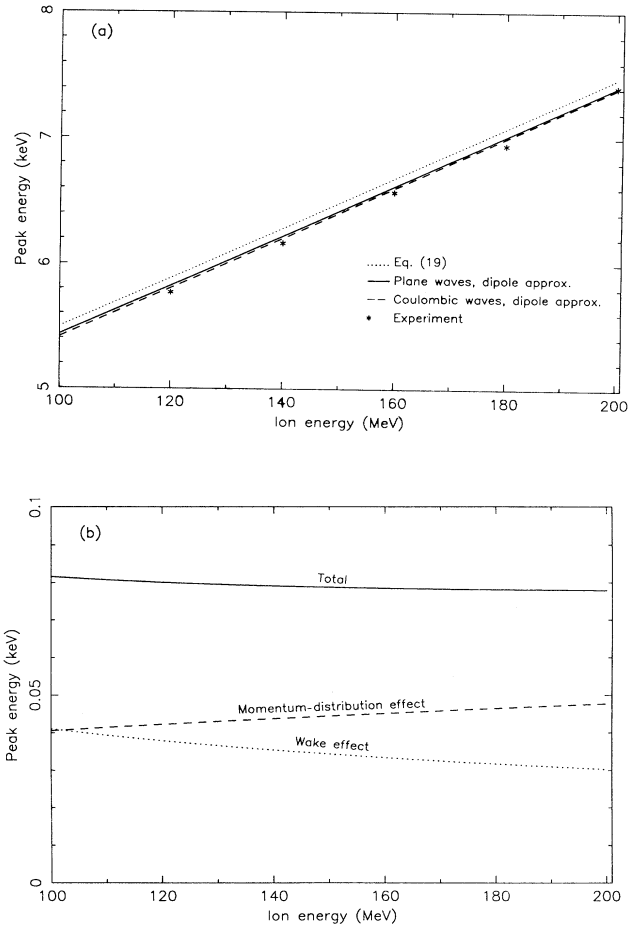

FIG. 5. (a) Peak-energy positions of the average DIMFP per unit energy and unit solid angle calculated from Eq. (47), as a function of the energy of bombarding ions, for $b_{min}=0.1$ Å and the distance-dependent local DIMFP's of Eqs. (35) (solid line) and (45) (dashed line). Also shown are the REC energies of Eq. (19) (dotted line) and the measured peak energies of Ref. 13 (cross points). (b) Calculated energy deficit, as a function of the energy of bombarding ions (solid line). The dashed and dotted lines represent the contribution to the energy deficit from the broadening of the initial momentum distribution and from wake corrections to the binding energy of the captured electron, respectively.

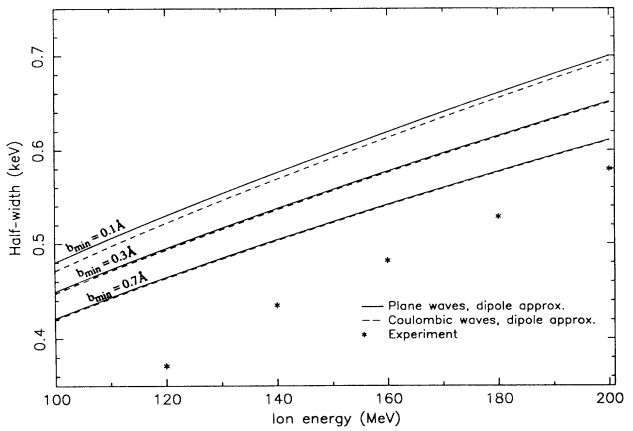

FIG. 6. Half widths calculated from Eq. (47) as a function of the incident ion energy, with minimum impact parameters from 0.1 to 0.7 Å. The local DIMFP's for capture of electrons in a given part of the solid are calculated from Eqs. (35) (solid lines) and (45) (dashed lines). Also shown are the measured widths of Ref. 13 (cross points).

Finally, we have calculated the REC differential cross sections per target atom and unit solid angle, by dividing the average DIMFP of Eq. (47) by the atomic density of the solid and integrating numerically over the photon energy. Figure 7 shows results from Vane *et al.*[13] measurements of *K*-shell REC yield from bare sulfur ions channeled in silicon, together with our calculated differential cross sections. Notice that in the range of energies of interest in REC experiments when initial Coulombic wave functions are used (dashed curves), the differential cross section decreases somewhat more rapidly, as the energy increases, than when plane waves are employed (solid curves); this may explain the fact that REC peak energies calculated making use of the full Coulomb potential be-

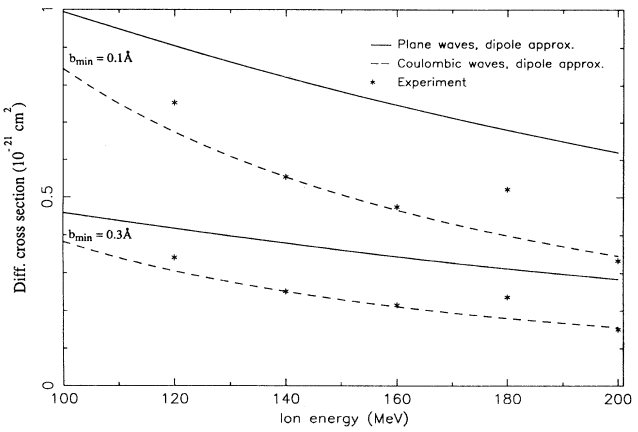

FIG. 7. REC differential cross sections plotted as a function of ion energy calculated from Eq. (47) with the local DIMFP's of Eqs. (35) (solid curves) and (45) (dashed curves), for $b_{min}=0.1$ Å and $b_{min}=0.3$ Å. These results are compared with the experimental data of Ref. 13 (cross points) normalized at 140 MeV.

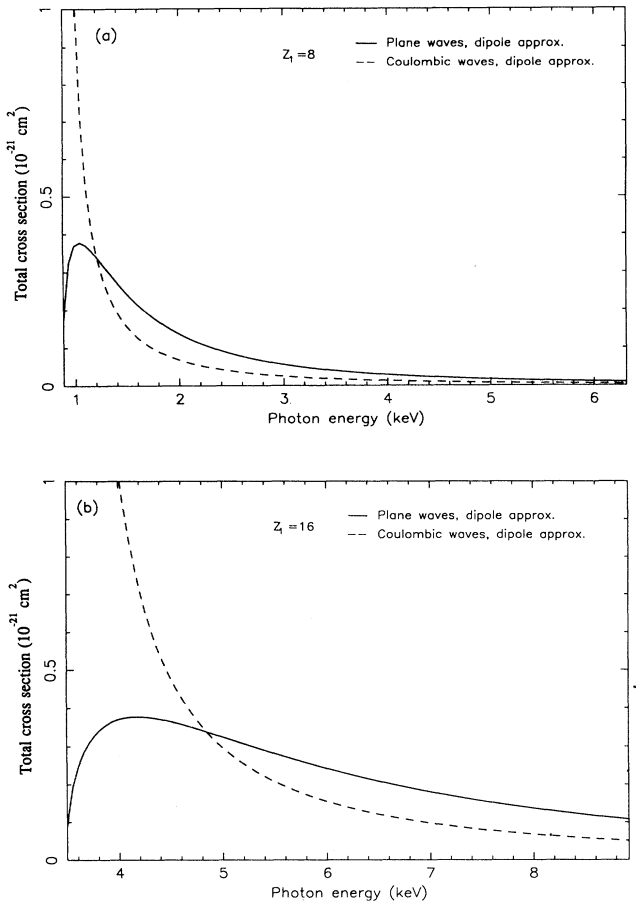

FIG. 8. Total recombination cross sections calculated from Eq. (48) (solid curves) and from Eq. (49) (dashed curves), as a function of emitted photon energy, for $Z_1=8$ [Fig. 8(a)] and $Z_1=16$ [Fig. 8(b)].

come slightly smaller.

Such differences between differential cross sections per unit target atom and solid angle also exist in the well-known total cross sections for recombination. These are[19]

$$\sigma=\frac{2^6}{3}\frac{1}{c^2}\frac{2\pi}{c}\frac{(-\nu_f)^{5/2}(\nu+\nu_f)^{1/2}}{\nu^3} \tag{48}$$

and

$$\sigma=\frac{2^7\pi}{3}\frac{1}{c^2}\frac{2\pi}{c}\frac{(-\nu_f)^3}{(\nu+\nu_f)\nu^2}f(\sqrt{-\nu_f/(\nu+\nu_f)}) , \tag{49}$$

when plane waves and when Coulombic waves are used to represent target electrons, respectively; in these expressions $1/c^2$ is the classical electron radius, $2\pi/c$ the Compton wavelength of the electron, and ν_f and ν represent the frequency of the captured electron and the emitted radiation frequency, respectively.

Figure 8 shows plots of the total recombination cross sections calculated from Eqs. (48) (solid curves) and (49) (dashed curves) against the emitted photon energy, for different values of the bombarding ion charge: $Z_1=8$ [Fig. 8(a)] and $Z_1=16$ [Fig. 8(b)]. Notice that although at high energies the cross section can be determined approximately using the Born approximation, that is, assuming that the target electrons are initially free, for energies of interest here the introduction of the bare Coulomb potential gives rise to a faster decrease of the cross section as the photon energy is increased. This is specially true for high Z_1; however, this effect seems to be not appreciable at high velocities when the charge of the bombarding ion becomes smaller, as one might expect.

IV. CONCLUSIONS

We have used a statistical local-density approach to model the capture of electrons by swift ions channeling in solids. Our results tend to confirm the deficit in REC photon energies observed by Vane *et al.* This deficit originates in two different physical mechanisms, both of which become more important with decreasing impact parameter of the ion relative to atoms in the solid. These are (a) the width of the distributions in momentum of electrons in the solid, and (b) the depolarizing effect of the ion's wake on the binding energy of the captured electron. Use of Coulombic initial-state wave functions tends to result in improved agreement with experimental REC energies.

ACKNOWLEDGMENTS

This research has been sponsored by the Universidad del País Vasco/Euskal Herriko Unibertsitatea, by Eusko Jaurlaritza, by the Office of Health and Environmental Research, U.S. Department of Energy, under Contract DE-AC05-840R21400 with Martin Marietta Energy Systems, Inc., and by the U.S.–Japan Cooperative Science Program of the National Science Foundation, Joint Research Project No. 87-16311/MPCR-168.

[1]H. W. Schnopper, H. D. Betz, J. P. Delvaille, K. Kalata, A. R. Sohual, X. Jones, and M. E. Wesner, Phys. Rev. Lett. **29**, 898 (1972).

[2]P. Kienle, M. Klaber, B. Pouh, R. M. Diamond, F. S. Stevens, E. Grosse, M. R. Moier, and B. Proctel, Phys. Rev. Lett. **31**, 1099 (1973).

[3]H. W. Schnopper, J. P. Delvaille, K. Kalata, A. R. Solival, M. Abdulwahab, K. W. Jones, and H. E. Wegner, Phys. Lett. **47A**, 61 (1974).

[4]J. S. Briggs and K. Dettman, Phys. Rev. Lett. **33**, 1123 (1974).

[5]H. W. Shnopper, H. D. Betz, and J. P. Delvaille, in *Atomic Collisions in Solids,* edited by S. Datz, B. R. Appleton, and C. D. Moak (Plenum, New York, 1975), Vol. II. p. 481.

[6]B. R. Appleton, T. S. Noggle, C. D. Moak, J. A. Biggerstaff, S. Datz, H. F. Krause, and M. D. Brown, in *Atomic Collisions in Solids* (Ref. 5), p. 499.

[7]B. R. Appleton, R. H. Ritchie, J. A. Biggerstaff, T. S. Noggle, S. Datz, C. D. Moak, and H. Verbeek, J. Nucl. Mater. **63**, 513 (1976).

[8]R. Shakeshaft and L. Spruch, Rev. Mod. Phys. **51**, 369 (1979).

[9]B. R. Appleton, R. H. Ritchie, J. A. Biggerstaff, T. S. Noggle, S. Datz, C. D. Moak, H. Verbeek, and V. N. Neelavathi, Phys. Rev. B **19**, 4347 (1979).

[10]J. E. Miraglia, Phys. Rev. A **32**, 2702 (1985).

[11]S. Andriamonje, M. Chevallier, C. Cohen, J. Dural, M. J. Gaillard, R. Genre, M. Hage-Ali, R. Kirsch, A. L'Hoir, B. Mazuy, J. Mory, J. Moulin, J. C. Poizat, J. Remillieux, D. Schamaus, and M. Toulemonde, Phys. Rev. Lett. **59**, 2271 (1987).

[12]J. E. Miraglia, R. Gayet, and A. Salin, Europhys. Lett. **6**, 397 (1988).

[13]C. R. Vane, S. Datz, P. Dittner, J. Giese, J. Gomez del Campo, N. Jones, H. Krause, P. D. Miker, H. Schone, and M. Schulz (unpublished).

[14]R. Shakeshaft and L. Spruch, Phys. Rev. Lett. **38**, 175 (1977).

[15]P. A. M. Dirac, *The Principles of Quantum Mechanics,* 4th ed. (Clarendon, Oxford, 1958), Chap. 10.

[16]L. I. Schiff, *Quantum Mechanics* (McGraw-Hill, New York, 1968), Chap. 4.

[17]R. H. Ritchie, W. Brandt, and P. M. Echenique, Phys. Rev. B **14**, 4808 (1976); P. M. Echenique, R. H. Ritchie, and W. Brandt, Phys. Rev. B **20**, 2567 (1979).

[18]L. D. Landau and E. M. Lifshitz, *Course of Theoretical Physics: Quantum Electrodynamics* (Pergamon, New York, 1982), Vol. 4, p. 165.

[19]H. A. Bethe and E. E. Salpeter, *Quantum Mechanics of One- and Two-Electron Atoms* (Academic, New York, 1957), p. 322.

[20]J. M. Pitarke and R. H. Ritchie (unpublished).

[21]T. C. Tucker, L. D. Roberts, C. W. Nestor, T. A. Carlson, and F. B. Malik, Phys. Rev. **178**, 988 (1969). We are grateful to Dr. C. W. Nestor for furnishing the data to us.